AFRL-ML-WP-TR-2001-4139

EFFECTS OF COMPRESSIVE STRESS ON FLUORESCENT PENETRANT INDICATIONS OF FATIGUE CRACKS IN TITANIUM

John C. Brausch
AFRL/MLSA
Building 652, Room 122
2179 12th Street
Wright-Patterson AFB, OH 45433-7718

Noel A. Tracy
Universal Technology Corporation
1270 North Fairfield Road
Dayton, OH 45432-2600

March 2001

FINAL REPORT FOR PERIOD 01 OCTOBER 1998 – 31 MARCH 2001

MATERIALS AND MANUFACTURING DIRECTORATE
AIR FORCE RESEARCH LABORATORY
AIR FORCE MATERIEL COMMAND
WRIGHT-PATTERSON AIR FORCE BASE, OH 45433-7750

NOTICE

USING GOVERNMENT DRAWINGS, SPECIFICATIONS, OR OTHER DATA INCLUDED IN THIS DOCUMENT FOR ANY PURPOSE OTHER THAN GOVERNMENT PROCUREMENT DOES NOT IN ANY WAY OBLIGATE THE US GOVERNMENT. THE FACT THAT THE GOVERNMENT FORMULATED OR SUPPLIED THE DRAWINGS, SPECIFICATIONS, OR OTHER DATA DOES NOT LICENSE THE HOLDER OR ANY OTHER PERSON OR CORPORATION; OR CONVEY ANY RIGHTS OR PERMISSION TO MANUFACTURE, USE, OR SELL ANY PATENTED INVENTION THAT MAY RELATE TO THEM.

THIS REPORT IS RELEASABLE TO THE NATIONAL TECHNICAL INFORMATION SERVICE (NTIS). AT NTIS, IT WILL BE AVAILABLE TO THE GENERAL PUBLIC, INCLUDING FOREIGN NATIONS.
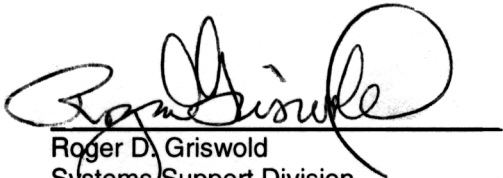
THIS TECHNICAL REPORT HAS BEEN REVIEWED AND IS APPROVED FOR PUBLICATION.

John C. Brausch
Materials Integrity Branch
Systems Support Division

Michael F. Hitchcock
Materials Integrity Branch
Systems Support Division

Roger D. Griswold
Systems Support Division
Materials and Manufacturing Directorate

Do not return copies of this report unless contractual obligations or notice on a specific document require its return.

REPORT DOCUMENTATION PAGE

1. AGENCY USE ONLY (Leave blank)	2. REPORT DATE March 2001	3. REPORT TYPE AND DATES COVERED Final Report, 10/01/1998 – 03/31/2001

4. TITLE AND SUBTITLE EFFECTS OF COMPRESSIVE STRESS ON FLUORESCENT PENETRANT INDICATIONS OF FATIGUE CRACKS IN TITANIUM	5. FUNDING NUMBERS C: F33615-97-C-5640 PE: 62102F PR: 4349 TA: S1 WU: 01
6. AUTHOR(S) John C. Brausch (AFRL/MLSA) Noel A. Tracy (UTC)	

7. PERFORMING ORGANIZATION NAME(S) AND ADDRESS(ES) AFRL/MLSA Building 652, Room 122 2179 12th Street Wright-Patterson AFB, OH 45433-7718 Universal Technology Corporation 1270 North Fairfield Road Dayton, OH 45432-2600	8. PERFORMING ORGANIZATION REPORT NUMBER UTC-S435-778

9. SPONSORING / MONITORING AGENCY NAME(S) AND ADDRESS(ES) MATERIALS AND MANUFACTURING DIRECTORATE AIR FORCE RESEARCH LABORATORY AIR FORCE MATERIEL COMMAND WRIGHT-PATTERSON AIR FORCE BASE, OH 45433-7750 POC: John Brausch, AFRL/MLSA, (937) 656-9151	10. SPONSORING / MONITORING AGENCY REPORT NUMBER AFRL-ML-WP-TR-2001-4139

11. SUPPLEMENTARY NOTES

12a. DISTRIBUTION / AVAILABILITY STATEMENT Approved for public release; distribution unlimited.	12b. DISTRIBUTION CODE

13. ABSTRACT *(Maximum 200 Words)*

Although it has been generally accepted that compressive stress adversely affects the fluorescent penetrant indications of fatigue cracks, published supporting data was lacking. To begin to fill this data void, five titanium specimens containing low cycle fatigue cracks were repetitively processed with a standardized liquid penetrant procedure after known stresses had been applied. A fixture was designed to apply known amounts of compressive stress on the cracked surfaces over the range of 0 to 63.5 ksi. The penetrant indications were measured and analyzed with two independent techniques. Eddy current inspection data were also generated for comparison with the penetrant data. The liquid penetrant indications began to diminish immediately with the application of compressive stress. On the other hand, the amplitudes of the eddy current indications remained the same over the entire range of applied stress.

14. SUBJECT TERMS Fluorescent penetrant inspection, fatigue cracks, nondestructive evaluation (NDE)	15. NUMBER OF PAGES 40
	16. PRICE CODE

17. SECURITY CLASSIFICATION OF REPORT Unclassified	18. SECURITY CLASSIFICATION OF THIS PAGE Unclassified	19. SECURITY CLASSIFICATION OF ABSTRACT Unclassified	20. LIMITATION OF ABSTRACT SAR

TABLE OF CONTENTS

LIST OF FIGURES

LIST OF TABLES

ACKNOWLEDGEMENTS

EXECUTIVE SUMMARY

Although it has been generally accepted that compressive stress adversely affects the fluorescent penetrant indications of fatigue cracks, published supporting data was lacking. To begin to fill this data void, five titanium specimens containing low cycle fatigue cracks were repetitively processed with a standardized liquid penetrant procedure after known stresses had been applied. A fixture was designed to apply known amounts of compressive stress on the cracked surfaces over the range of 0 to 63.5 ksi. The penetrant indications were measured and analyzed with two independent techniques. Eddy current inspection data were also generated for comparison with the penetrant data. The liquid penetrant indications began to diminish immediately with the application of compressive stress. On the other hand, the amplitudes of the eddy current indications remained the same over the entire range of applied stress.

1. INTRODUCTION

1.1 Background

The effectiveness (sensitivity) of fluorescent penetrant inspection is affected by many variables. These variables include the degree of inspection process control, various human factors, and conditions of the inspected component such as material type, surface condition, surface cleanliness and stress state. Although it is generally accepted that compressive stress adversely affects the fluorescent penetrant indications of fatigue cracks, published supporting data is lacking. Conditions of particular concern are compressive stresses due to shot-peening as well as residual compressive fields resulting from plastic deformation during loading in service.

1.2 Objectives of the Program

- Generate data to show the effects of applied surface compressive stress on fluorescent liquid penetrant indications of low cycle fatigue cracks in metal specimens representative of material used in turbine engines.

- Evaluate the data to determine the compressive stress at which crack closure inhibits the entry of sufficient fluorescent penetrant to produce a detectable indication of a crack.

- Evaluate the effect of compressive stress on eddy current inspection results using the same specimens and applied stresses.

- Evaluate the use of image analysis methods to assess penetrant performance quantitatively.

1.3 Scope of Work

- Obtain specimens containing low cycle fatigue cracks from the available population and characterize the cracks with optical and liquid penetrant inspection techniques.

- Design and procure loading fixtures for applying equal compressive surface stress perpendicular to the crack opening of each specimen.

- Calibrate the loading fixtures to facilitate quick application of a known stress prior to processing the specimens with liquid penetrant.

- Develop a liquid penetrant inspection technique for processing the specimens in their respective loading fixtures.

- Develop a procedure for measuring and analyzing the fluorescent penetrant indications.

- Develop an eddy current inspection technique.

- At ascending levels of stress measure the response of each crack to the applied fluorescent penetrant and eddy current inspection techniques.

- Thermally stress relieve the specimens to eliminate residual stresses due to the manufacturing process.

- After thermal stress relief, repeat the fluorescent penetrant process and the measurements of crack responses at ascending levels of stress.

- Repeat the previous step except modify the penetrant and emulsifier dwell times.

- Process and analyze the measurement data.

2. Test Specimens

2.1 Description

Titanium- and nickel-alloy specimens were sought in order to match the materials used in turbine engines. Low cycle fatigue cracks with depths in the range of 0.020 to 0.035 inch were desired. These depths represented the required detection threshold for the turbine engines. Previous experience dictated that specimens approximately 6 inches long by 1 inch wide by 0.25 inch thick are both sufficient and convenient. Through a contact at Sandia National Laboratories five titanium (Ti-6Al-4V) specimens that met these preferred characteristics were obtained.[1]

The specimens (figure 1) had been cut from ¼-inch thick Ti-6Al-4V rolled plate procured to ASTM B 265, Grade 5. To speed crack growth, the specimens were excised from the plate such that the longitudinal grain of the material was parallel to the 1-inch edges of the specimen. Spot weld damage was introduced as a stress riser at the center of one 1- by 6-inch surface. Low cycle fatigue cracks were generated at room temperature using a load frame fitted with a three-point bend fixture. Cracks were grown parallel to the one-inch edge of each specimen. After a crack had been introduced into a specimen, the surface was machined to remove the spot-weld damage. A surface grinder was used as the final machining operation to produce a surface finish of 32 RMS microinches maximum.

The crack lengths were verified by applying image processing measurement techniques to magnified images (70x to 100x) produced on a metallograph. The crack sizes are listed in table 1.

Table 1. Dimensions of low cycle fatigue cracks

Specimen Number	Measured Length (inch)	Crack Depth (inch)*
17	0.018	0.0084
63	0.036	0.0154
41	0.039	0.0184
44	0.048	0.0240
53	0.056	0.0247

*Based upon theoretical two-to-one aspect ratio and a correction for thickness reduction which occurred during grinding to remove the respective spot welds used as a stress risers to initiate crack growth.

2.2 Characterization and Preparation

The cracks were characterized further by processing the five unstressed specimens with fluorescent liquid penetrant and measuring the luminance of the resulting crack indications. The technique for measuring luminance is discussed in section 7.1. The fluorescent penetrant indications were discontinuous, some having the appearance of two separated bright dots. Scanning electron micrographs revealed that final surface

grinding at the conclusion of the specimen manufacturing process had smeared metal across the crack openings. These results dictated a light surface etch.

Kroll's etchant, consisting of 1 ml of hydrofluoric acid, 2 ml of nitric acid and 100 ml of distilled water, was applied with a swab for approximately 30 seconds. After etching, the fluorescent penetrant indications were continuous, although some had the appearance of a dumbbell, typical of cracks in surfaces under compressive stress.

X-ray diffraction techniques were used to make residual stress measurements of each specimen at a location approximately half way between one end of each crack and the long edge of the respective specimen. These initial residual stress results are listed in table 2. As suspected from the dumbbell shape of some fluorescent penetrant indications, the residual stress measurements indicate compressive stress. The residual compressive stresses were probably due to the manufacturing process used to produce the raw material. The specimens were originally cut from rolled rather than mill annealed plate. The presence of the initial residual stresses necessitated the need to compare penetrant indication results obtained before and after thermal stress relief. The process employed for the specimen stress-relief is discussed in section 8. Thermal stress relief was conducted only after an initial characterization of the penetrant indications at ascending levels of stress was completed.

Table 2. Residual stress summary

	Longitudinal Residual Stress (ksi)	
Specimen Number	Before Annealing	After Annealing
17	-50.9 $\pm$ 4.5	4.2 $\pm$ 1.3 0.3 $\pm$ 2.1
63	-40.6 $\pm$ 2.3	-5.8 $\pm$ 1.8 -3.8 $\pm$ 1.2
41	-38.3 $\pm$ 4.5	0.9 $\pm$ 1.9 -0.1 $\pm$ 1.5
44	-35.7 $\pm$ 3.3	-4.1 $\pm$ 1.5 1.7 $\pm$ 1.5
53	-60.3 $\pm$ 3.6	-2.8 $\pm$ 1.6 -3.1 $\pm$ 1.4

3. LOADING FIXTURE

3.1 Fabrication

A stainless steel loading fixture (figure 2) was designed so that compressive stress could be easily applied to the cracked surface of a specimen and the stressed specimen could be processed with fluorescent penetrant materials in accordance with the standardized processing procedure. It was desired to apply the maximum possible stress at the crack location while not exceeding the elastic limit load (90 ksi) at any point on the specimen. The fixture allows each specimen to be clamped in place so that the fatigue crack on the upper surface is one inch away from the beveled edge of the clamping plate. This spacing and the bevel were designed to allow access with an X-ray beam if it was desired to make residual stress measurements at the crack location with the specimen in the fixture under stress. The end view of the fixture in figure 2 shows

the cap screw used to bend the specimen and apply compressive stress to the upper surface of the specimen.

Five identical fixtures were manufactured, one for each specimen. Before calibration the fixtures were marked to enable reproducible placement of each specimen in its respective fixture during the study.

3.2 Calibration

Each fixture was individually calibrated with its specimen as follows. First, a strain gage was applied to each specimen half way between one end of each crack and the closest long edge. One at a time each fixture with its respective specimen was clamped to a solid base. An electronic displacement gage was used to measure the displacement of the end of the specimen as the cap screw was turned (see figure 3). The strain and displacement data were collected automatically by computer and tabulated as surface compressive stress versus displacement. Limiting the applied stress at the fulcrum of the bent specimen to 90 ksi resulted in a maximum stress of up to 70 ksi at a crack one inch from the fulcrum.

Up to 500 data points were generated for each specimen. The maximum applied stress level that was common to all five specimens was found to be 63.5 ksi. Starting at this level a convenient interval of 5 ksi was chosen for selecting the stress levels and the respective displacements at which the specimens would be processed with liquid penetrant. The result was 13 levels of applied stress, the lowest being 3.5 ksi.

4. PROCESSING AND MEASUREMENT PROTOCOL

4.1 Basic Cycle

Each of the following steps was always applied to the specimens in the same order.

- Insert each specimen into its loading fixture.

- Apply the respective nondestructive inspection process.

- Repeat the above two steps at applied compressive stress levels of 3.5 ksi, and then at 5 ksi intervals up to 63.5 ksi.

4.2 Fluorescent Penetrant Inspection Protocol

- Apply the standard fluorescent penetrant inspection process.

- Measure each fluorescent penetrant indication: directly with a photometer and indirectly by acquiring a digital image and analyzing the image.

- Remove the specimens from the loading fixtures and clean the specimens.

5. STANDARDIZED FLUORESCENT PENETRANT INSPECTION PROCESS

Each specimen was processed with a standardized fluorescent penetrant inspection procedure. The penetrant processing parameters (table 3) match those specified in the penetrant materials specification, *SAE AMS 2644, Inspection Material, Penetrant*[2] except for slight modifications to facilitate handling the specimens in the loading fixtures. The fluorescent penetrant materials used were Sherwin RC-77 liquid penetrant, Magnaflux ZR-10B hydrophilic emulsifier and ZP-4B dry developer. These materials

were from the group of reference materials used for qualifying candidate products in accordance with AMS 2644. The RC-77/ZR-10B penetrant system is the reference system for the highest level of sensitivity (Level 4).

In the course of the study, the specimens were processed with fluorescent penetrant through the range of stress levels three times. First, data was gathered on the specimens as received, that is, with residual stress. Second, data was gathered after eliminating the inherent residual stresses through thermal stress relieving (annealing). Third, data was gathered on the stress relieved specimens using modified penetrant and emulsifier dwell times (table 4). The modified dwell times more closely represent processes used in the propulsion industry. Specifically, the penetrant dwell time was increased to 30 minutes and the emulsifier dwell was decreased to 2 minutes.

Table 3. Fluorescent penetrant processing parameters

Penetrant Dwell	Apply penetrant to center of each specimen with a transfer pipette and dwell 5 minutes
Prewash	Wipe off excess surface penetrant with a clean dry cloth (deviation from normal spray wash)
Emulsification[1]	Invert fixture and immerse specimen in emulsifier unagitated 5 minutes
Wash[2]	Spray 2 minutes
Dry	Place in recirculating oven 5 minutes[3]
Developer	Dip and dwell 5 minutes
[1] Emulsifier concentration: 20 percent. [2] Water: 25 psi (172 kPa), 70°F±5 (21°C±3). [3] Oven: 135°F±5 (57°C±3).	

Table 4. Modifications to fluorescent penetrant processing parameters

Penetrant Dwell	Increase to 30 minutes
Emulsification	Decrease to 2 minutes

6.   SPECIMEN CLEANING

The specimens were cleaned between each processing interval by removing the specimen from the fixture and washing with a soft brush using detergent and warm water. Clean water rinse and towel drying followed. The specimens were then placed in a rack and dipped in methanol to remove excess water. After allowing the methanol to evaporate in air for one minute, the specimens were placed in a container of HCFC 141B and ultrasonically agitated for ten minutes. Following a one-minute drying period in a recirculating oven at 135°F $\pm$ 5° (57°C $\pm$ 3°) to volatize all the solvent, the specimens were ready for processing.

This cleaning process has proved successful during repetitive penetrant inspection processing of similar specimens for material qualification in accordance with AMS 2644. When not being used, the specimens were stored in a container of HCFC 141B.

7. MEASUREMENT OF FLUORESCENT PENETRANT INDICATIONS

Two methods were employed for measurement of fluorescent penetrant indications. One method, employing luminance measurements, was selected because it has been traditionally used to classify the sensitivity of penetrant materials in accordance with SAE AMS 2644. The second method employed computer analysis of digital images to quantify the areas and intensities of the penetrant indications. Measurements were always made in the same order according to specimen number.

7.1   Luminance (Photometric Brightness)

A Photo Research® PR-1500 Spectra® Spotmeter® with a photopic filter (figure 4), provided a digital luminance value calibrated in foot-Lamberts. The circular aperture of the instrument projected onto the specimen surface provided a measurement field-of-view approximately 0.02 by 0.06 inch. A lamp with two integrally filtered fluorescent tubes provided the ultraviolet (UV-A) radiation. The UV-A radiation intensity at the specimen surface (nominally 1650 μW/cm^2) was measured with a digital radiometer.

Two luminance measurements were taken for each penetrant indication. One measurement was made with a crack indication within the field of view. A second measurement was made adjacent to the indication to record fluorescent background. The fluorescent background measurement was subtracted from the first measurement to give the recorded value for indication luminance. This correction was made because the crack indications did not completely fill the field of view of the photometer, so it was necessary to subtract any contribution due to background. This is the type of data traditionally used to evaluate the relative sensitivities of liquid penetrant materials as part of the qualification testing performed in accordance with AMS 2644.

7.2   Area and Integrated Intensity

Images of the fluorescent penetrant indications were captured at 70x magnification with an Olympus® Video Microscope Model DVM-1 and subsequently analyzed with Image-Pro Plus™ software. Figure 5 illustrates the equipment configuration for these measurements used to acquire the images. The near ultraviolet radiation (UV-A) was provided through a waveguide by an independent source. Prior to capturing each set of images, the radiation intensity at the crack location was set at 12,500 μW/cm^2 with the aid of the digital radiometer. This higher UV-A intensity was required due to the lower sensitivity of the camera optics compared to that of the photometer.

After each set of images of the five crack indications was captured at a stress level, additional images of two fluorescent features on a visual-comparator card were also captured. These images were used as references for UV-A intensity and spatial calibration. An image of one feature, a 1/16-inch diameter fluorescent spot, was measured to detect any drift in the intensity of the ultraviolet radiation from set to set and correct the indication intensity data if necessary. An image of the second feature, a two-millimeter section of a linear scale, was captured to calibrate the image analysis software.

Image analysis was performed with computer software to measure specific attributes of the fluorescent indications. The analysis steps were as follows: a) calibrate the image intensity and scale using the respective reference images, b) outline the edges of

indications using an empirically determined intensity threshold, and c) calculate the indication attributes (area, integrated intensity, etc).

For the purposes of this study, all of the individual segments of each indication were considered part of the indication. The image background was eliminated from the calculated image attributes by establishing an intensity threshold. Only pixels at or above this threshold value would contribute to the calculated attributes. The threshold value was empirically established by discriminating low intensity pixels that were not visually associated with the fluorescent indications at zero applied stress. This value effectively established the intensity threshold by which the edges of indications were automatically defined by a bright (red) line, illustrated in figure 7.

Several indications exhibited a segmented/discontinuous nature. For these indications the software drew an outline around each segment and tabulated the attribute values for each segment. The individual measured attributes were then combined to provide total attribute values for the entire indication. The attributes measured for each indication were area, length (major axis), width (minor axis), average pixel intensity and integrated intensity (average pixel intensity multiplied by area). The tabulated data was transferred to a spreadsheet for mathematical and graphical analysis.

Here, intensity is one component of the HIS (hue, saturation, intensity) color model and equals the mean of the red, blue and green components of the fluorescent indication. It would have been possible to calibrate the eight-bit intensity values in terms of a photometric unit such as luminance. However, since relative intensities were of primary importance in this study, the generic intensity range of 0 to 255 was used. Furthermore, the measure of average indication intensity is directly related to the thickness of the penetrant layer at the crack surface (assuming UV-A intensity and type of penetrant material are constant). Therefore, the value of integrated intensity (indication area x average pixel intensity) is a relative measure of the penetrant volume on the surface. By measuring the integrated intensity of each penetrant indication through successive loading conditions, the effect on the volume of penetrant that enters a fatigue crack can be monitored.

Within the respective spreadsheets the areas and integrated intensities of all segments were summed to obtain the total values for each indication. The length and width data were analyzed only for the condition of zero applied stress, and then only the largest segment of an indication was used for analysis. The small segments were generally interpreted as background noise. The measured lengths and widths were maximum values that tended to be skewed by the irregular shapes of the penetrant indications that could not be precisely reproduced. Segmentation of the indications at increased levels of applied stress rendered this data meaningless. Therefore, area data proved to be more reliable than length and width data for comparative analysis.

8. EDDY CURRENT INSPECTION PROCESS

An eddy current inspection was conducted to provide data to compare with that produced by the liquid penetrant inspection. A Staveley NDT-19e[II] instrument was set to operate at 2 MHz with an absolute shielded pencil probe. The initial calibration was performed with a titanium reference block containing EDM slots with depths of 0.2, 0.4 and 1.0 mm (0.008, 0.016 and 0.040 inch). Slight lift-off adjustments were made to

accommodate the alloy differences between the specimens and the reference block. At each applied stress level the probe was manually scanned over the specimens in their respective fixtures to obtain the maximum deflection of the flying spot on the impedance-plane instrument display from each crack.

The instrument display was adjusted so that the crack signal responses were indicated by positive vertical displacement of the flying spot. The maximum deflection, expressed as a percentage of full-screen height, was recorded as the eddy current indication amplitude.

9.   THERMAL STRESS RELIEVING (ANNEALING) THE SPECIMENS

Since the specimens initially contained residual compressive stresses, the effect of relieving that stress on fluorescent penetrant indications was evaluated. To measure the effect, the specimens were stress relieved and then the penetrant processing and image analysis were repeated. In preparation for stress relief, the specimens were thoroughly cleaned via a 30-minute ultrasonic agitation in acetone, individually wrapped in tantalum foil and encased in a quartz-glass tube. The glass vessel was then back filled with high purity argon and sealed. The vessels and specimens were then baked in an oven at $1000^{o}F$ for 10 hours. Repeating the X-ray diffraction residual stress measurements adjacent to each specimen crack demonstrated that the surface residual stresses were virtually eliminated (see table 2, column 3). After thermal stress relief, the measurements of penetrant indications at the ascending stress levels were repeated twice, once using the initial penetrant processing parameters (table 3) and the second time using modified dwell parameters (table 4).

10. RESULTS

10.1 Pre-anneal Fluorescent Penetrant Results

Images The pre-anneal crack indications are presented in column 1 of figures 7, 9, 11, 13, and 15. The calculated normalized integrated intensities are provided as the solid lines on the charts in figures 8, 10, 12, 14, and 16. All data in the charts have been normalized to the post-anneal values obtained at zero applied stress with unmodified penetrant processing. The intensity data representing the averages of for all five specimens is plotted in figure 17. The pre-anneal data demonstrates an immediate nonlinear degradation in penetrant indications at all applied loads. The penetrant indication integrated intensities dropped rapidly to approximately 50 percent of the unstressed values at approximately 22 ksi applied compressive stress (on average). At 30 ksi applied compressive stress the integrated intensity dropped to approximately 20 percent of the unstressed value (on average).

The indications continued to degrade rapidly, visually becoming very faint and discontinuous at the maximum applied compressive stress of 63.5 ksi. The crack indications from specimens #53 and #63 degraded to the point of becoming unmeasurable at 48.5 ksi and 28.5 ksi applied compressive stress respectively. However, the indications remained visible to the unaided human eye, although very dim, up to the maximum applied stress. Luminance measurements for these indications that could not be imaged were less than 1 foot-Lambert.

The photometric luminance data followed the same trends as the image analysis data.

10.2 Post-anneal Fluorescent Penetrant Results

Images of the post-anneal crack indications are presented in column 2 of figures 7, 9, 11, 13, and 15. The measurements of normalized integrated intensity are presented as the light (blue) bar data in charts contained in figures 8, 10, 12, 14, and 16. The intensity data representing the averages of all five specimens are provided in figure 17. The post-anneal results demonstrate a more gradual, linear degradation of the penetrant indications due to application of compressive stresses. The integrated intensity (area x average intensity) dropped to 50 percent of the unstressed value at approximately 38 ksi applied compressive (on average) and to 20 percent of the unstressed value at approximately 59 ksi applied compressive (on average).

All indications were detectable (measurable) through 63.5 ksi of applied compressive stress with the exception of specimen #63 which became discontinuous at 48.5 ksi and unmeasurable at 63.5 ksi of applied compressive.

Again, the photometric luminance data followed the same trends as the respective image analysis data.

Figure 18 compares the optical measurements of the crack lengths with the lengths of the fluorescent penetrant indications produced at zero applied stress before and after annealing. As expected the indications are longer than the cracks, and the indications after annealing are slightly longer than before. The length of the indication on specimen #63, as measured automatically with the image analysis software, was less than the actual crack length because the crack was partially closed. However, a manual measurement taken with the software, to include the barely perceptible indication at the right end of the crack (see figure 9), approximately equaled the crack length.

Figure 19 compares the areas of the indications before and after annealing. The increases in areas of 40 percent or more were primarily due to the increase in indication widths. The bar chart in the figure also shows that the increases in integrated intensities lagged the increases in areas especially for specimen #44, which had the largest increase in width. The crack indication for specimen #63 had the largest increase in area because it was partially closed before annealing.

10.3 Post-anneal Modified Dwell Results

Data for the modified dwell runs are presented as the dark (brown) bar data in charts contained in figures 8, 10, 12, 14, and 16. The smallest fatigue crack, #17, exhibited a decrease in integrated intensity at zero applied stress and virtually no change in integrated intensity, from previous runs at original dwell times, at the four highest load states (48.5, 53.5, 58.5, & 63.5 ksi). The other cracks generally exhibited increased intensities at all tested load levels. The data representing the averages for all five specimens is provided in figure 17, again as the dark (brown) bar data. The results demonstrate that, at zero applied stress, the extended penetrant dwell and decreased emulsifier dwell increased the integrated intensity an average of 27 percent. At the four highest applied stress states (48.5, 53.5, 58.5, & 63.5 ksi) the average indication integrated intensity increase by only 7 percent.

10.4 Eddy Current Results

The eddy current inspection results for the pre-annealed specimens (figure 20) demonstrate that no change in eddy current signal amplitude was encountered over the entire range of applied compressive stress. The respective eddy current indication amplitudes remained essentially constant regardless of the stress applied. Figure 21 shows that the eddy current data also correlates well with the penetrant indications and the measured crack lengths.

11. DISCUSSION

The results demonstrated the dramatic effect that a compressive stress field has on fatigue crack closure and the consequent diminished ability of penetrant to enter a fatigue crack. This effect, demonstrated as a significant degradation of the penetrant indications with increased compressive loading, is summarily and quantitatively presented in figure 17. Consider, for the moment, only the post-anneal results. The chart shows that on average the integrated intensity (average intensity x area) of the penetrant indications degraded to 50 percent of the unstressed value at approximately 38 ksi of applied compressive stress and to 20 percent at approximately 59 ksi. Compressive stresses resulting from shot peening or loading to the elastic limit (90 ksi) would be significantly higher. Therefore, one would expect the degradation of liquid penetrant indications to be considerably more pronounced than that observed in this experiment.

Significant variability in degradation of penetrant indications among the specimens was observed before annealing. This was most likely the result of variability in residual stresses through thicknesses of the respective specimens. Since it was not the purpose of this investigation to characterize this effect, X-ray diffraction residual stress profiles through the specimen thickness were not acquired. This profile data may have provided some insight into the inconsistent non-linear degradation before annealing.

The improvement in the penetrant indications after thermal stress relief is indicative of the effect that manufacturing-induced residual stresses may have on the closure of service-induced fatigue cracks. When the penetrant indications acquired at zero applied stress are compared, the integrated intensities before stress relief are 20 percent lower than after. This indicates that the volume of penetrant entering the cracks was reduced 20 percent due to the compressive field applied during manufacture from the rolling process.

Although increases in the integrated intensities of indications were observed after specimen annealing, no direct correlation could be drawn between these increases and the original residual compressive stresses. Again, this could be due to variations in the residual stress field through the thickness, errors associated with X-ray diffraction stress measurements or geometric effects due to crack shape. Since one would expect the residual compressive stresses resulting from shot peening, lance peening, or cold working to be significantly higher than the 30-60 ksi compressive stresses encountered on the surfaces of the specimens prior to annealing, further study using shot-peened specimens is warranted.

This study provided a measure of the relative effect of compressive stress on penetrant indication formation. However, the detectability of fatigue flaws under the influence of compressive stress was not characterized. This effect can only be assessed through a rigorous probability of detection (POD) study. Previous POD studies for fluorescent penetrant inspection have shown that fatigue cracks in an etched titanium plate on the order of 0.130 inch long can be detected with a 90 percent probability of detection with a 95 percent confidence.[3] Based on the results observed in this experiment, it is expected that the presence of compressive stresses would result in poorer fluorescent penetrant inspection performance.

Modified inspection process dwell times provided an overall improvement in the intensities of indications produced by small fatigue cracks. However, this improvement was minimal at high compressive stress states.

12. CONCLUSIONS

The data generated from this study substantiates the long known fact that surface compressive stress reduces the volume of liquid penetrant that enters a crack and, therefore, reduces the area and fluorescent intensity of the crack indication. This study was not designed to be a POD study. However, the study did establish that unknown stress conditions on the surfaces of parts will affect the intensity of a liquid penetrant indication and consequently the probability of detection in unpredictable ways.

Increasing the penetrant dwell time and simultaneously decreasing the emulsifier dwell time provides only a moderate improvement (27 percent) in indication integrated intensity at zero applied stress. At higher applied stress levels (48.5 to 63.5 ksi), the improvement is minimal (7 percent).

The amplitudes of eddy current signals from small fatigue cracks in titanium are not affected by applied compressive stresses.

Image-analysis software was successfully employed to provide quantitative measurements of areas and integrated intensities of penetrant indications.

13. RECOMMENDATIONS

Before fluorescent penetrant inspection is employed for the inspection of fracture critical components, specifically rotating engine components, consideration should be given to the stress fields within the inspection regions of interest. Fluorescent penetrant inspection should not be utilized for inspection of titanium (Ti-6AI-4V) components in the following situations: a) compressive surface stresses are expected to be above 40 ksi and b) detection of flaws with lengths of 0.060 inch or less is required. In these two situations, alternative inspection methods such as eddy current inspection should be considered.

Fluorescent penetrant inspection should not replace eddy current inspection without the benefit of well-designed POD studies on components containing residual stresses typical of in-service components.

Since only titanium specimens were used in this study, similar investigations with fatigue-crack specimens made of nickel-base alloys are required.
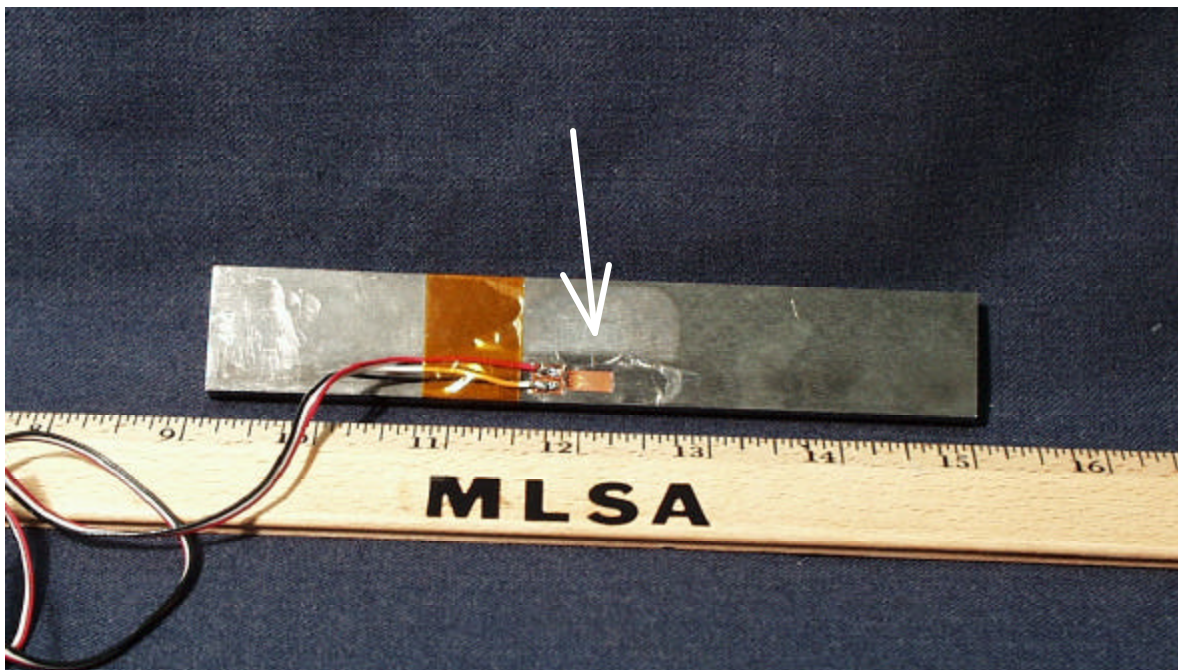
Figure 1. Ti-6Al-4V specimen with strain gauge attached. Arrow indicates location of fatigue crack.

Figure 2. Loading fixture with compressive stress applied to a specimen.
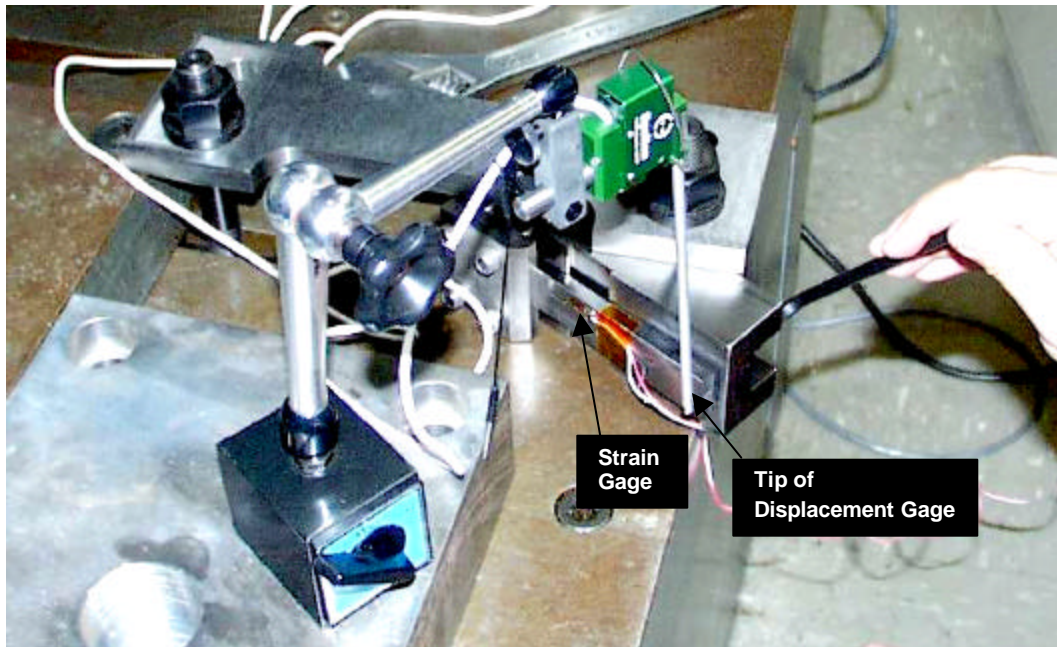
Figure 3. Apparatus for measuring strain versus displacement for independent calibration of each loading fixture.
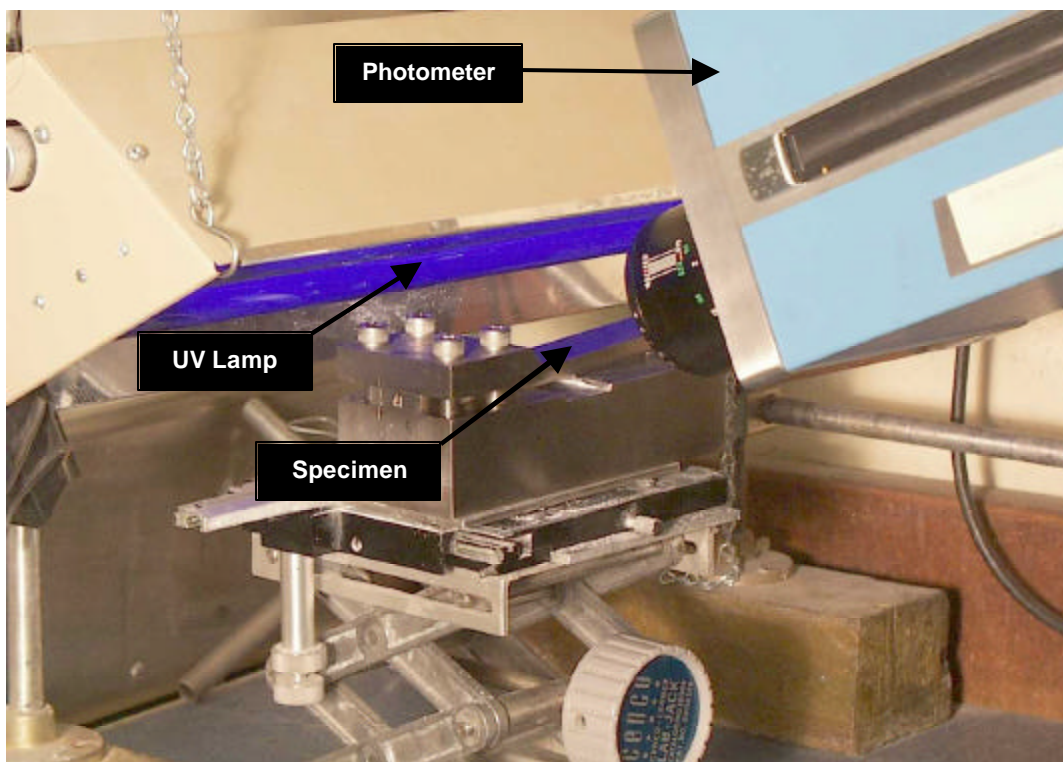

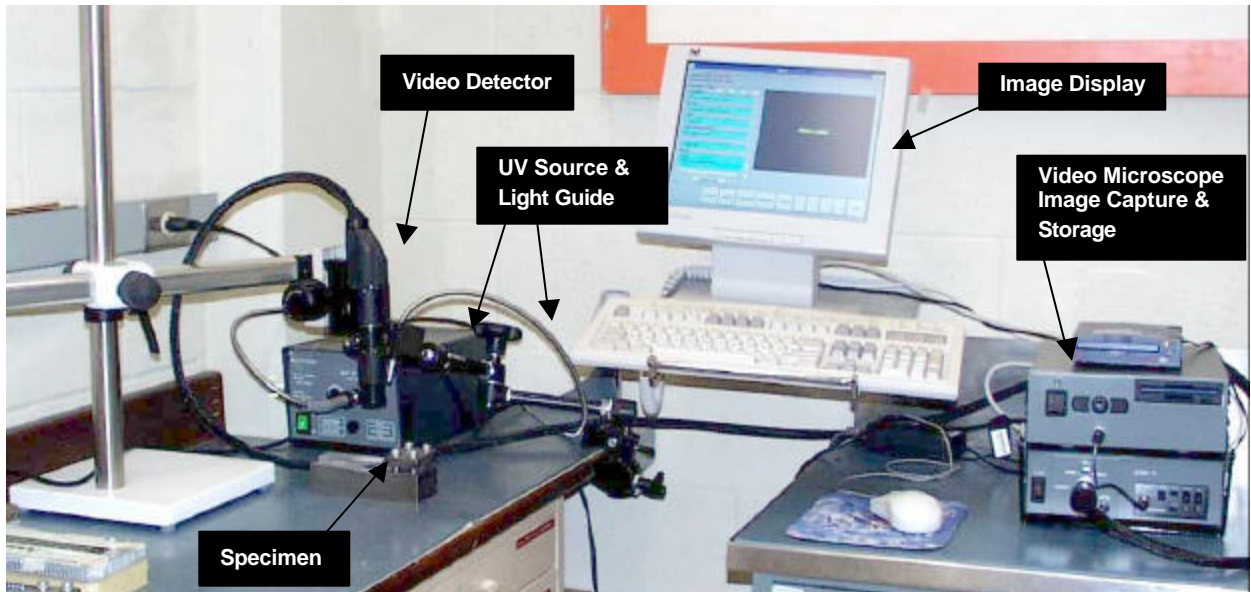**Figure 4. Equipment configuration for measuring luminance of fluorescent penetrant indications.**

Figure 5. Equipment configuration for acquiring digital images of fluorescent penetrant indications with the video microscope.
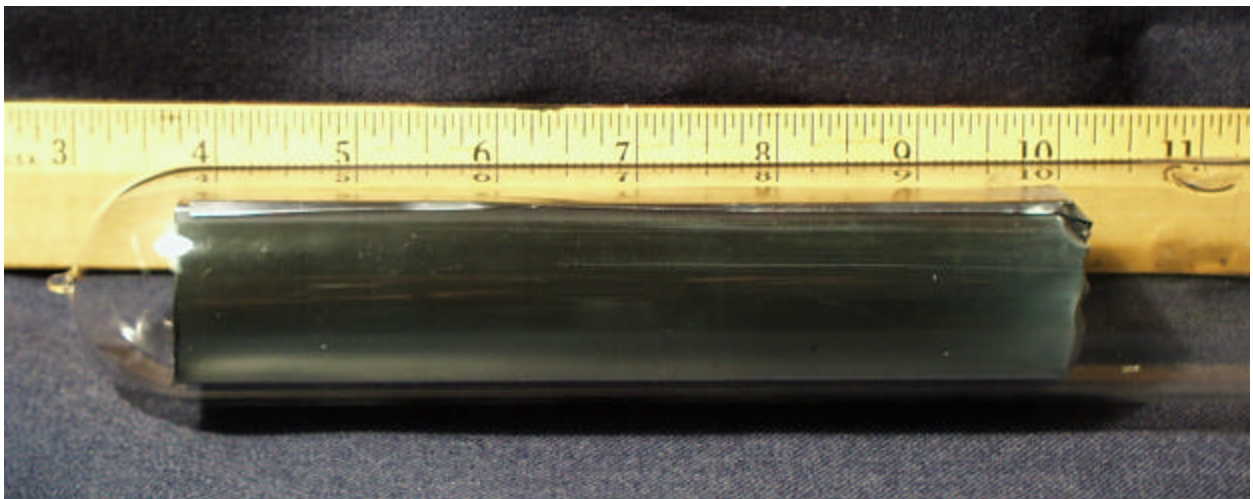
Figure 6. Specimen #57 prepared for annealing.
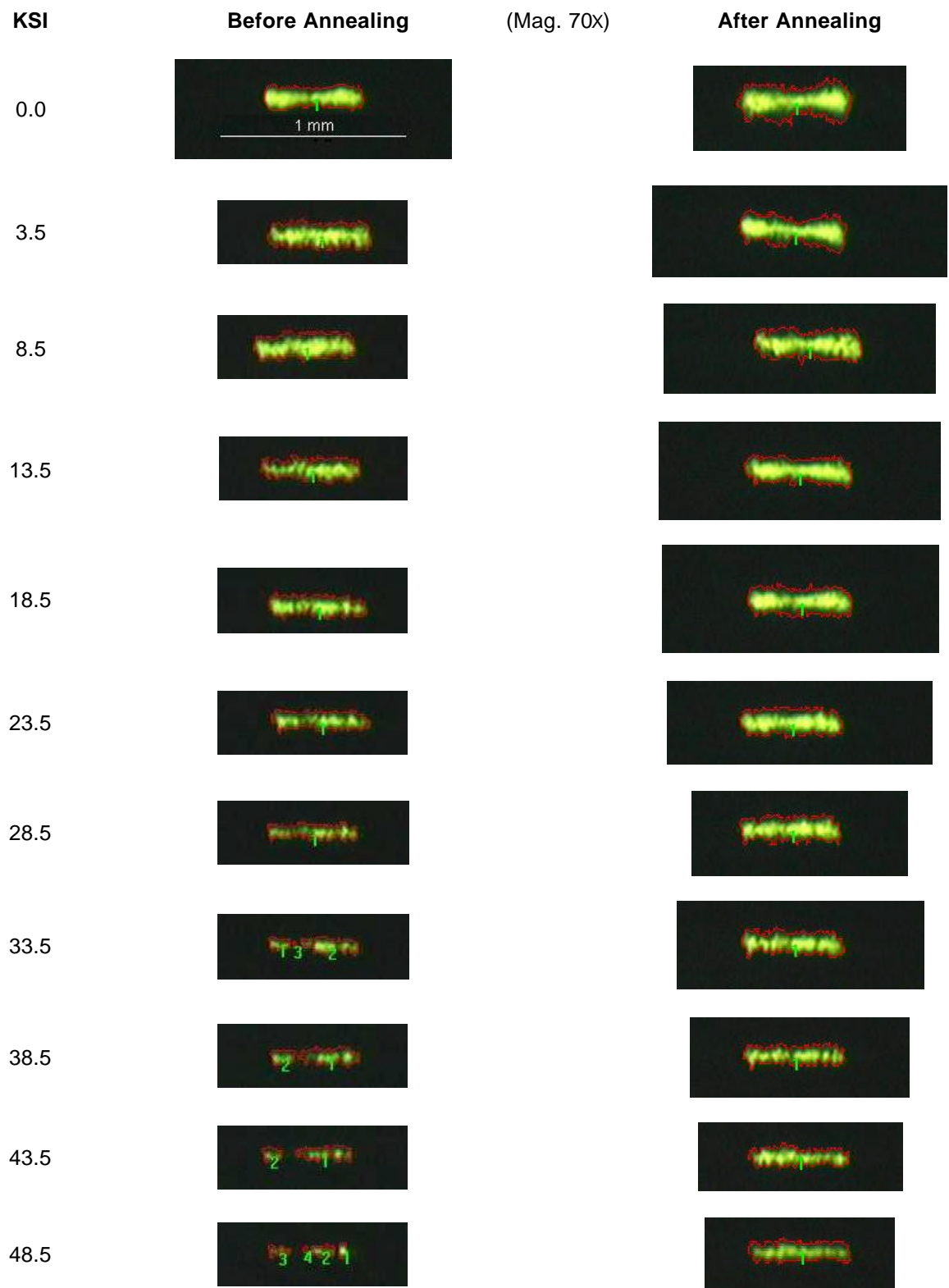
Figure 7. Fluorescent penetrant indications from the crack in specimen #17. (Part 1 of 2)

| KSI	Before Annealing	(Mag. 70x)	After Annealing
53.5			
58.5			
63.5			
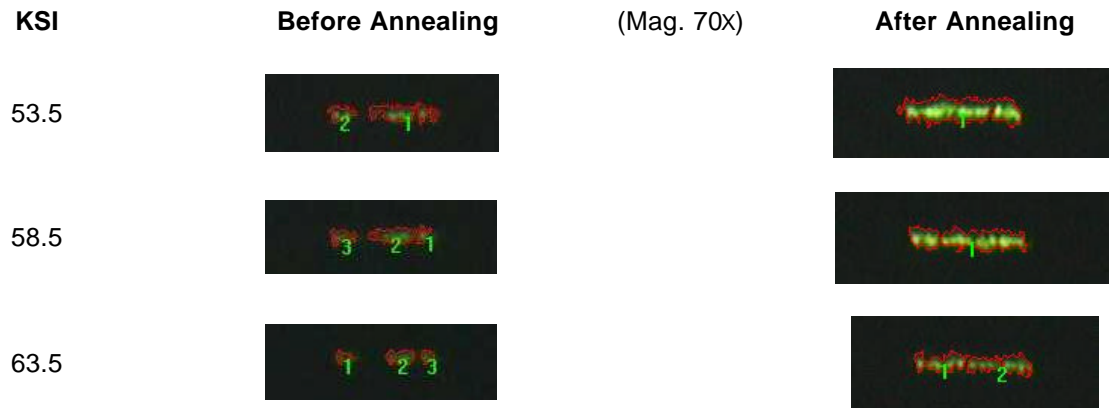
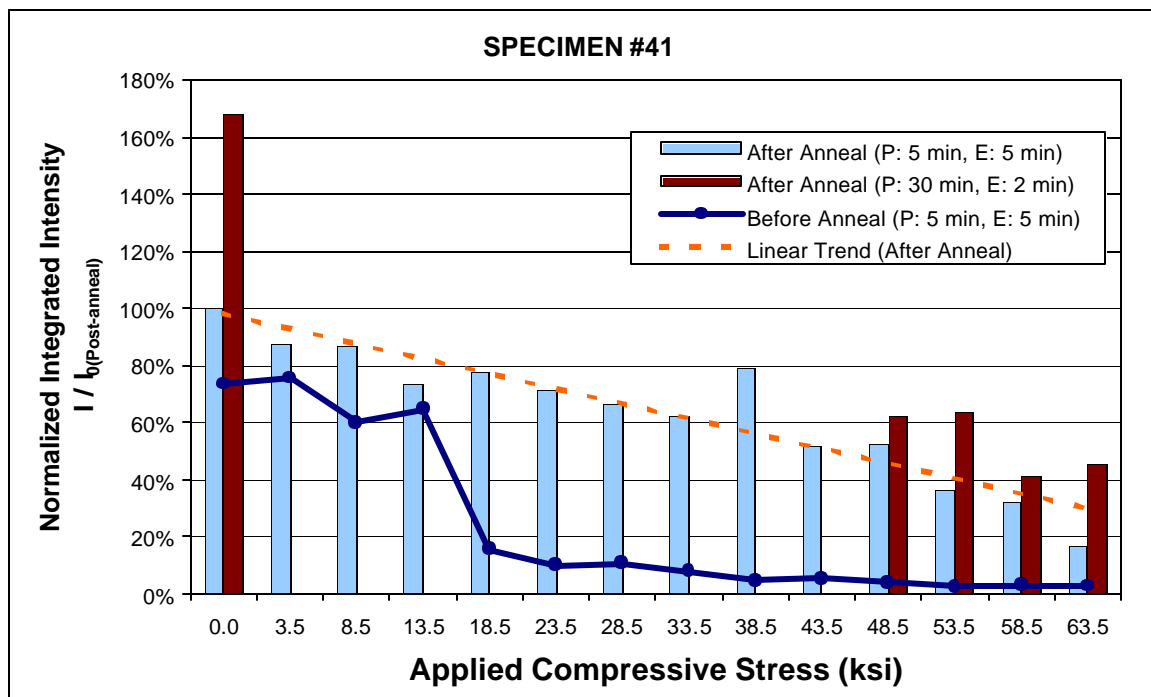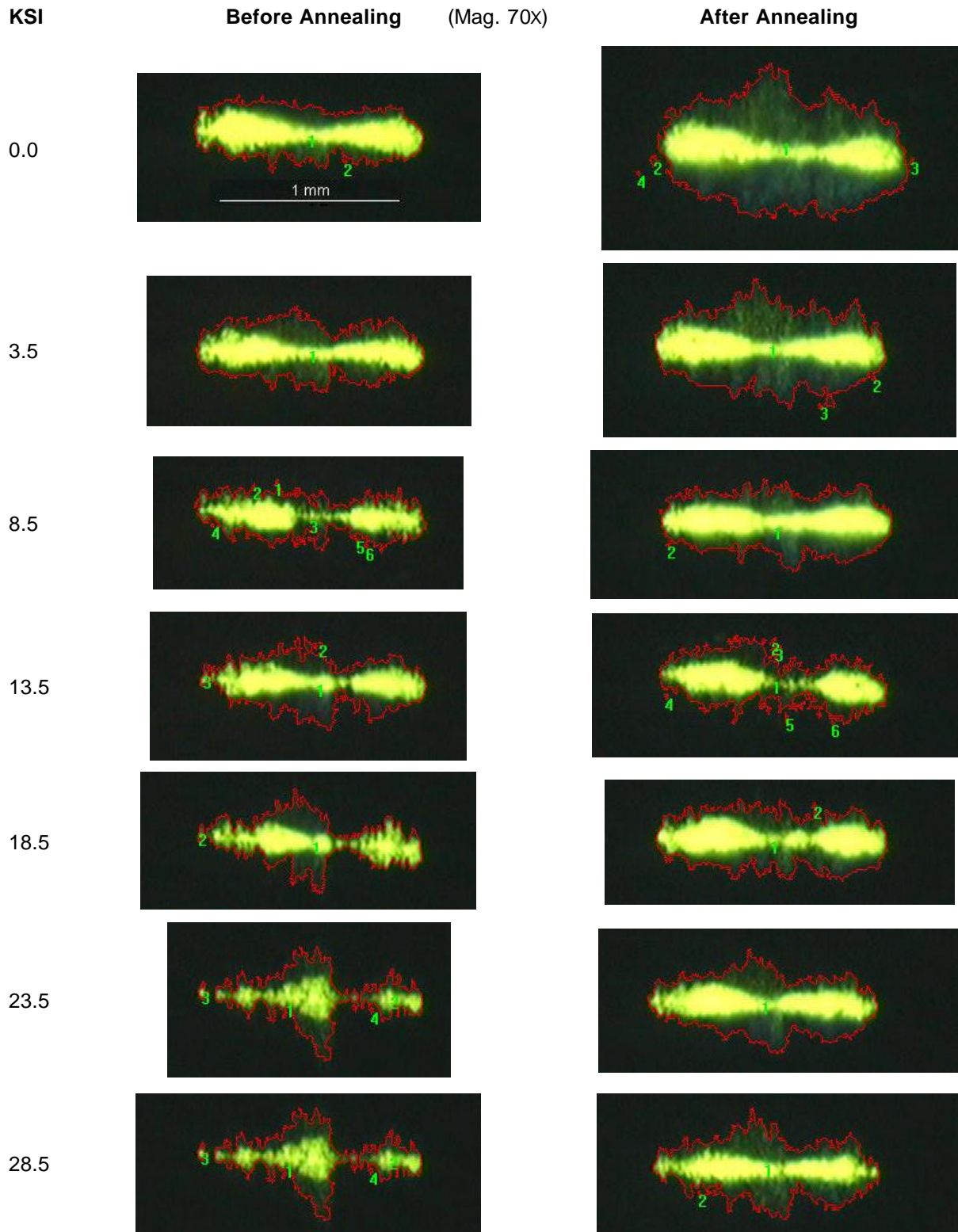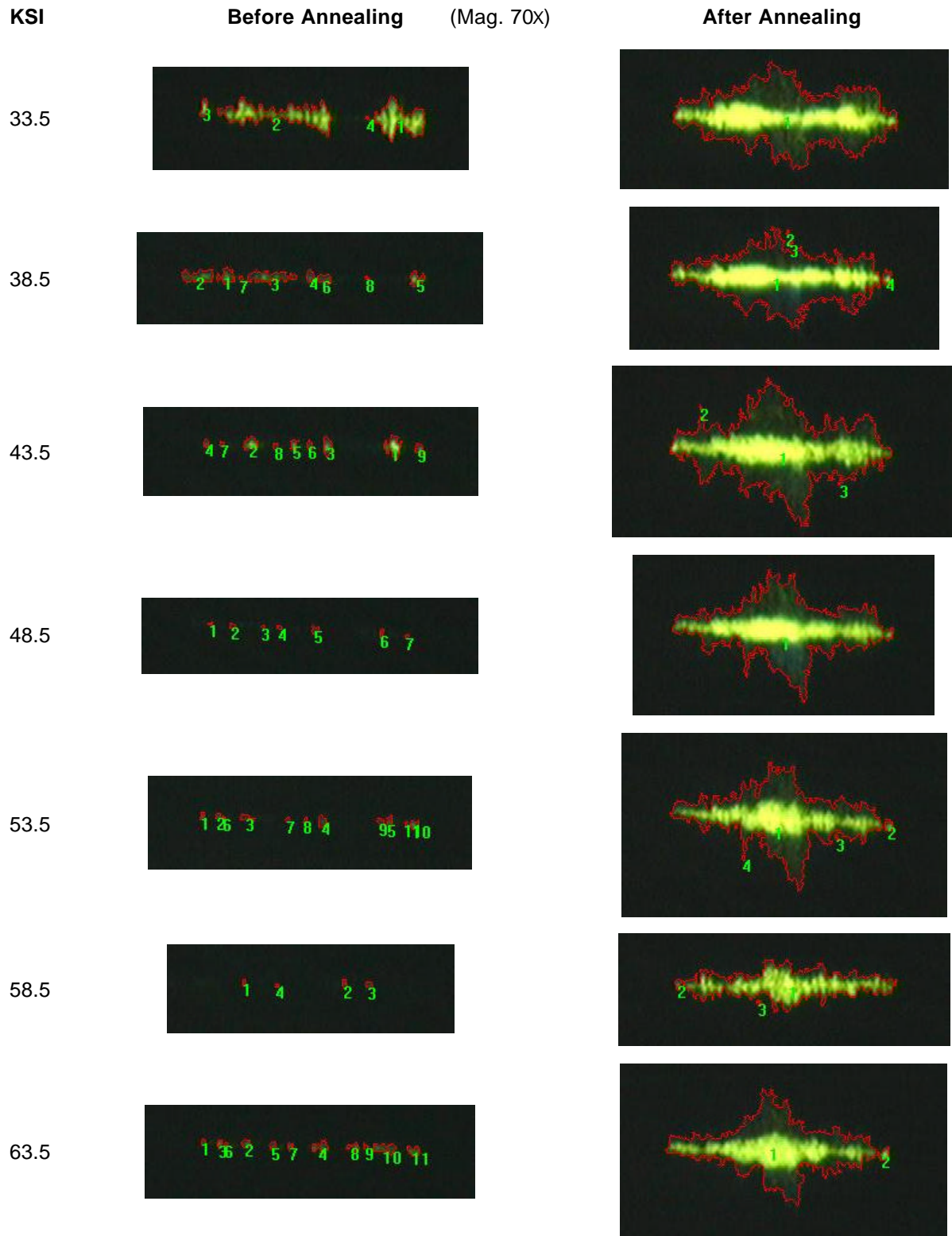**Figure 7. Fluorescent penetrant indications from the crack in specimen #17. (Part 2 of 2)**
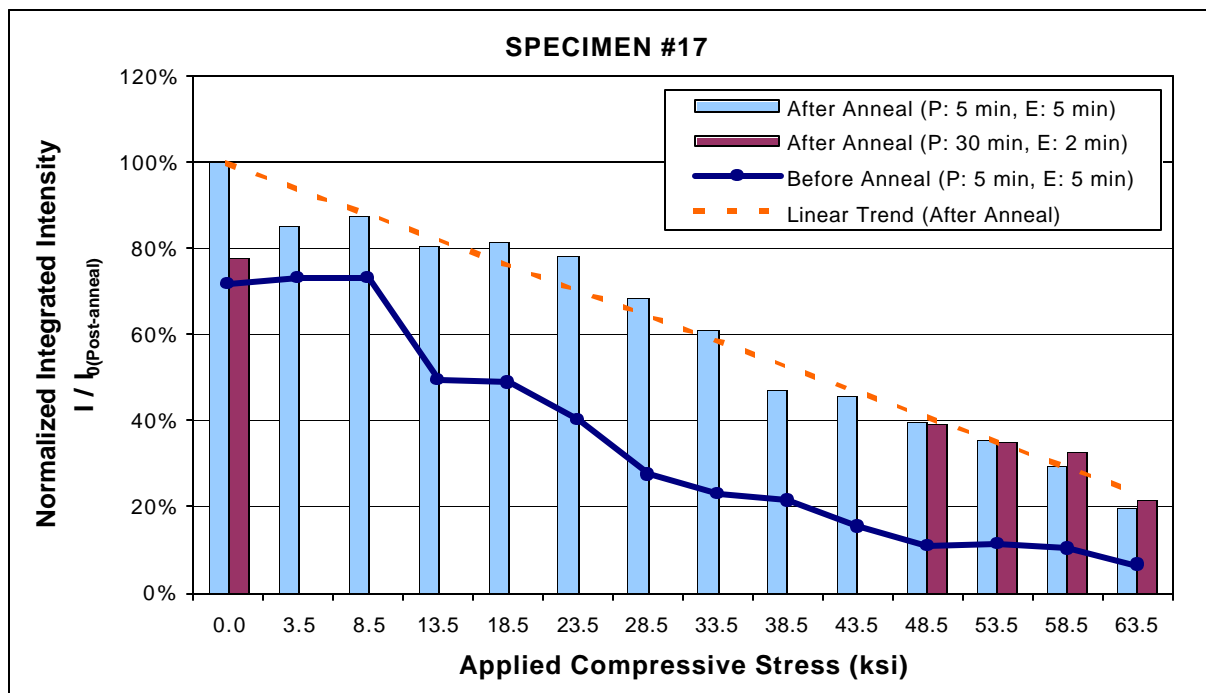
Figure 8. Integrated intensity of fluorescent penetrant indication of crack in specimen #17 normalized to the post-anneal integrated intensity at zero applied stress.
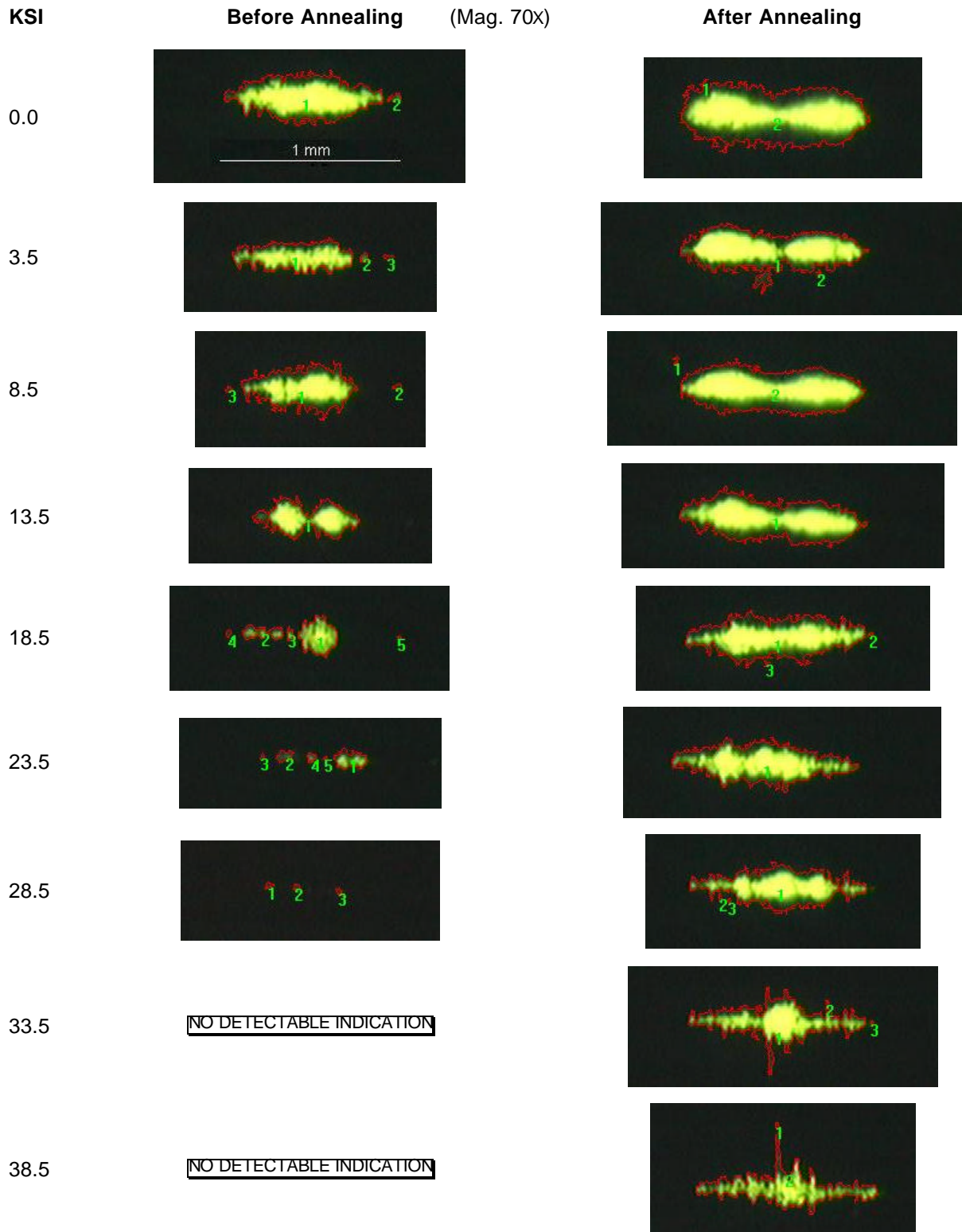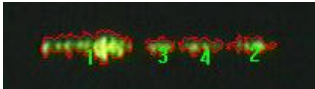
Figure 9. Fluorescent penetrant indications from the crack in specimen #63. (Part 1 of 2)

KSI	Before Annealing	(Mag. 70x)	After Annealing
43.5	NO DETECTABLE INDICATION		
48.5	NO DETECTABLE INDICATION		
53.5	NO DETECTABLE INDICATION		
58.5	NO DETECTABLE INDICATION		
63.5	NO DETECTABLE INDICATION		NO DETECTABLE INDICATION

Figure 9. Fluorescent penetrant indications from the crack in specimen #63. (Part 2 of 2)
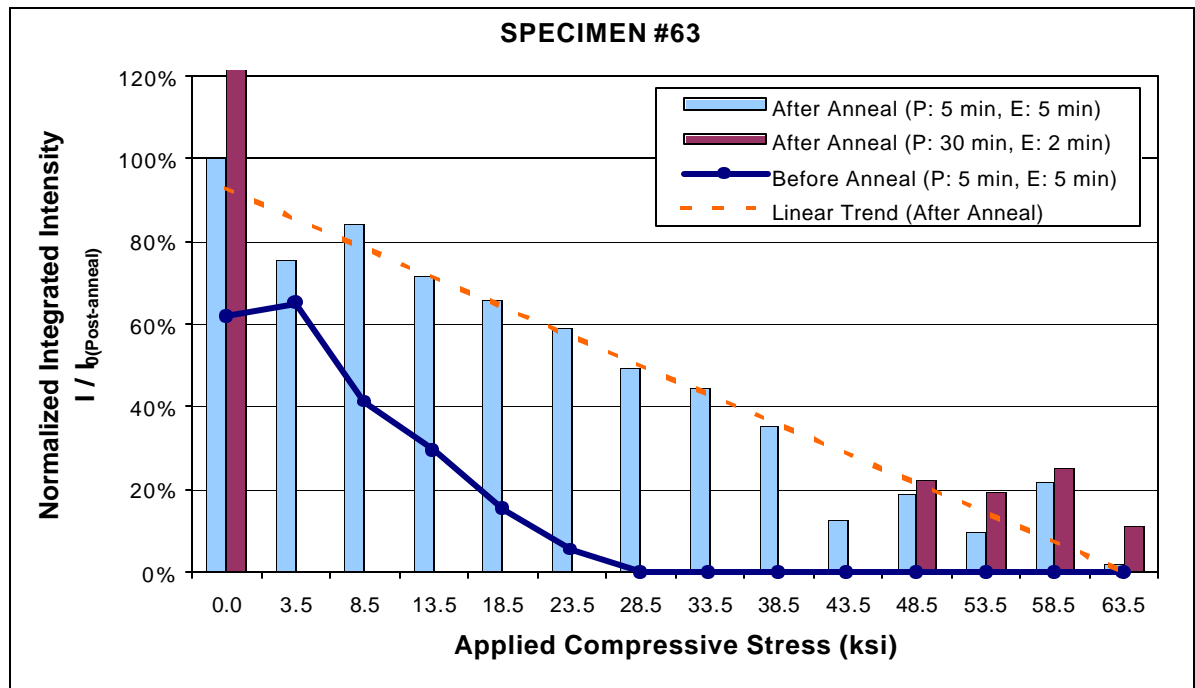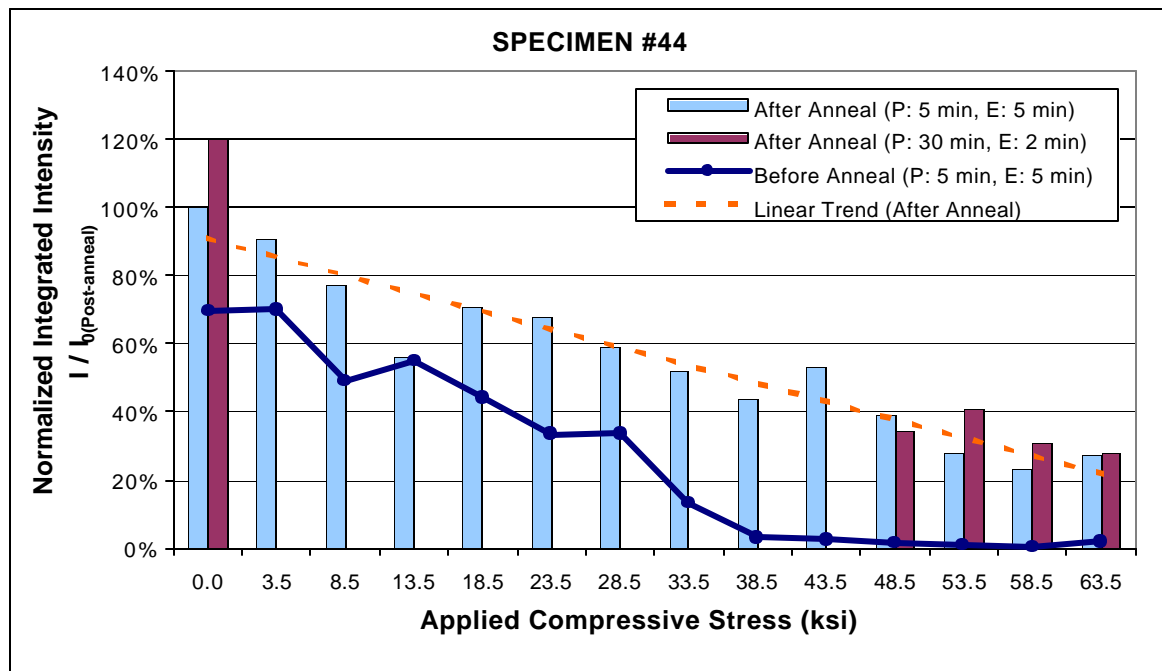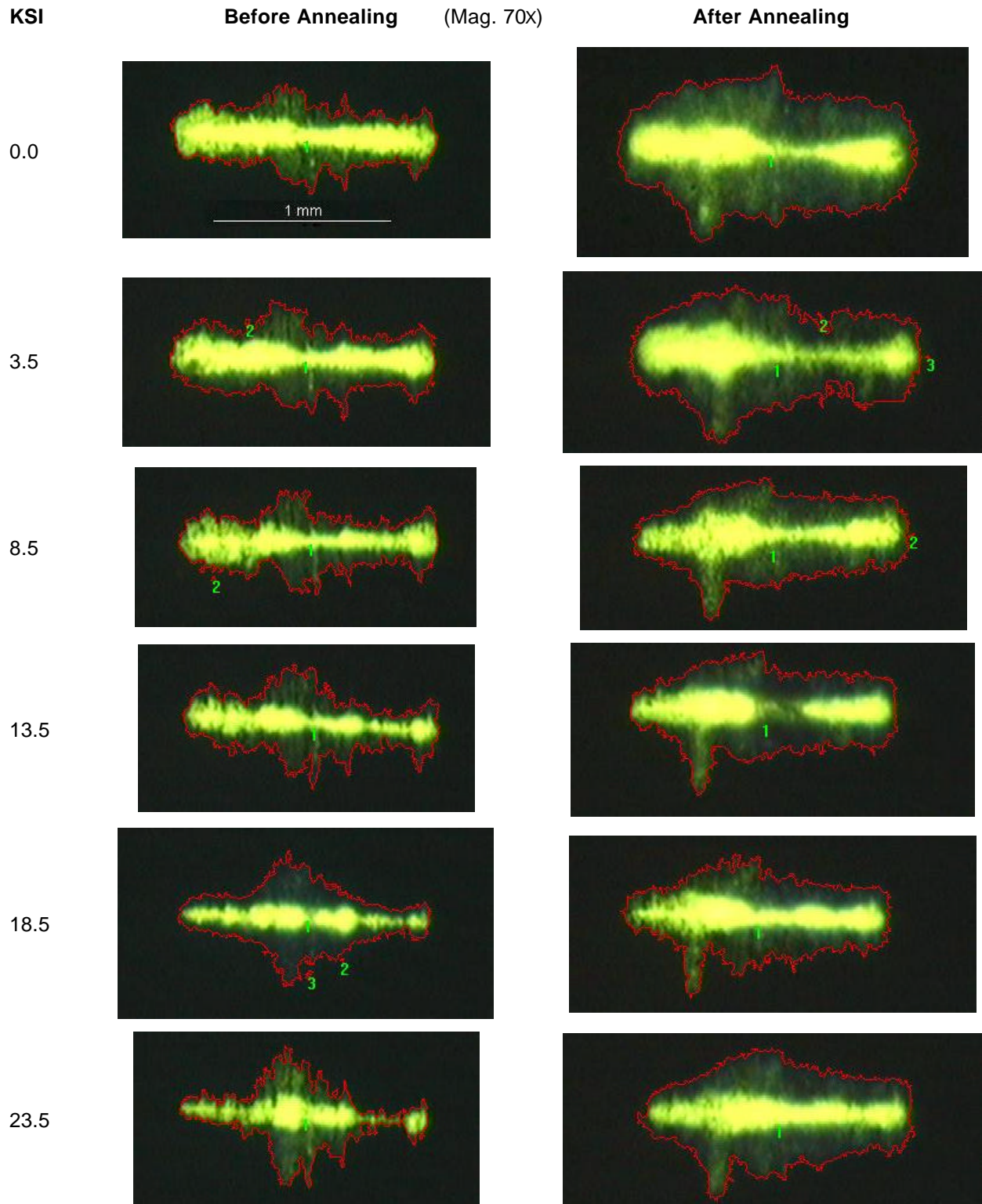

Figure 10. Integrated intensity of fluorescent penetrant indication of crack in specimen #63 normalized to the post-anneal integrated intensity at zero applied stress.
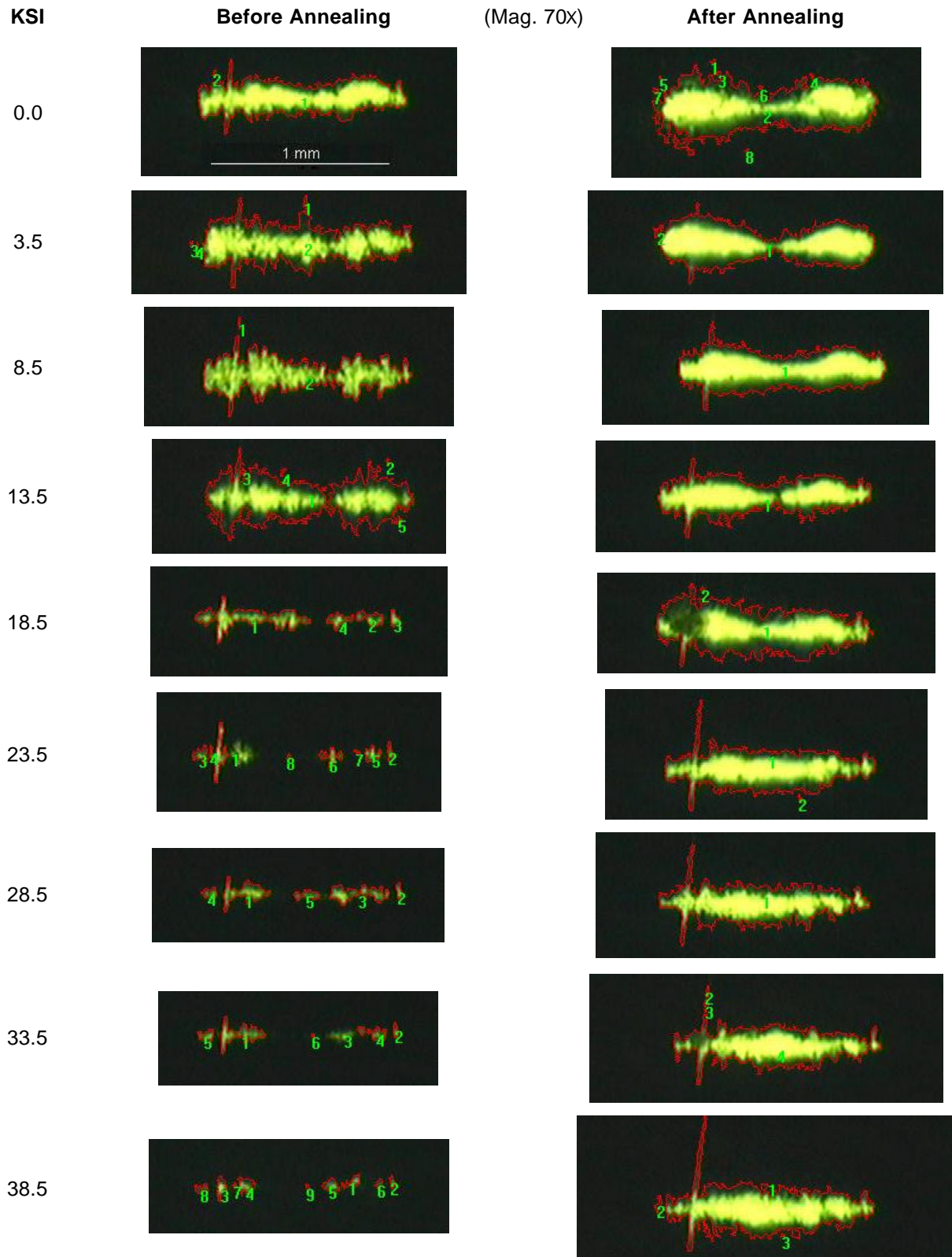
Figure 11. Fluorescent penetrant indications from the crack in specimen #41. (Part 1 of 2)
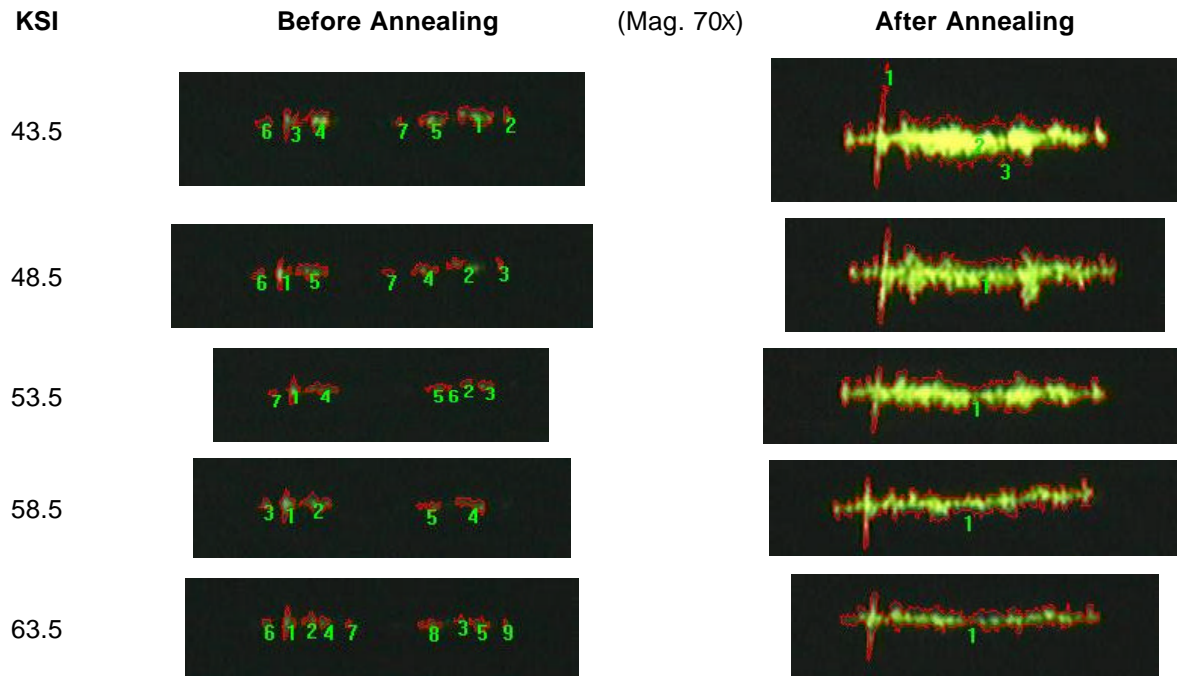
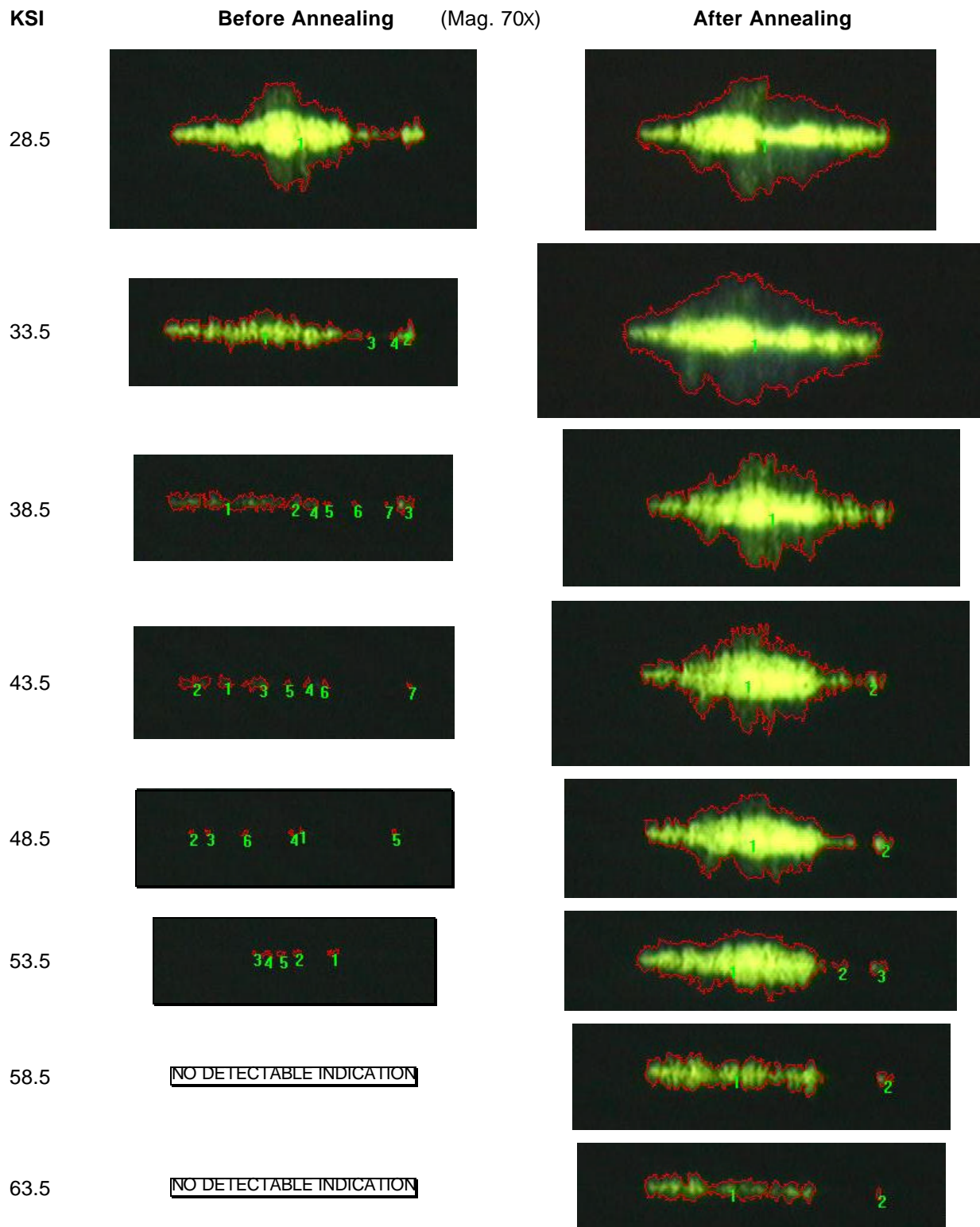**Figure 11. Fluorescent penetrant indications from the crack in specimen #41. (Part 2 of 2)**

Figure 12. Integrated intensity of fluorescent penetrant indication of crack in specimen #41 normalized to the post-anneal integrated intensity at zero applied stress.

Figure 13. Fluorescent penetrant indications from the crack in specimen #44. (Part 1 of 2)

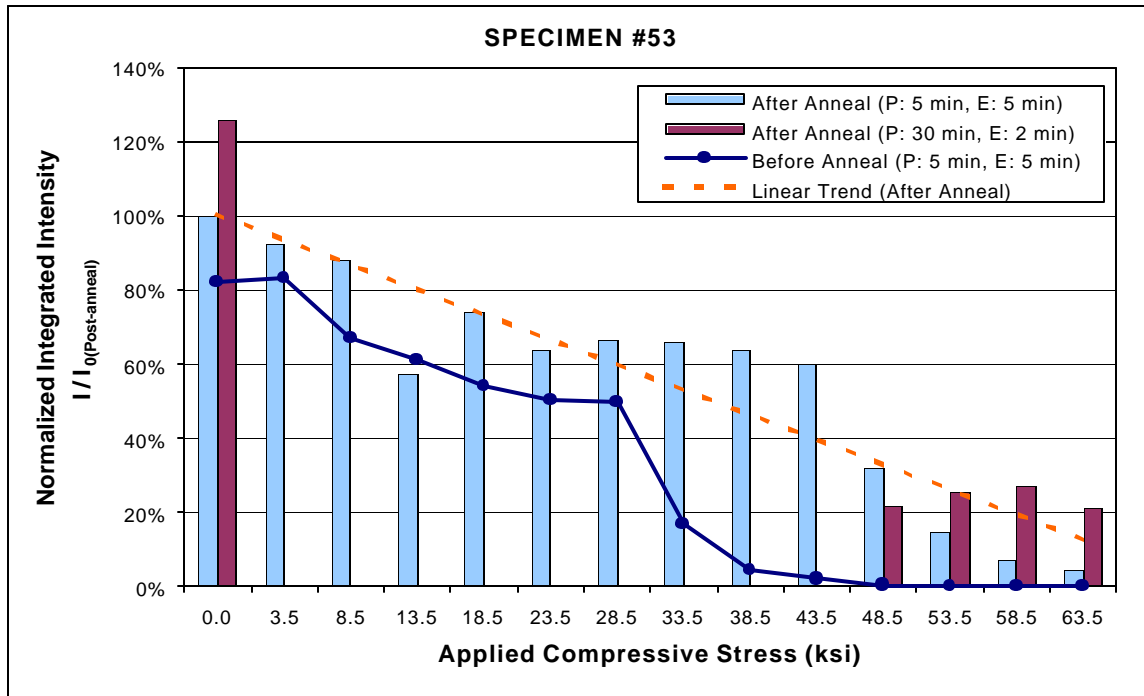**Figure 13. Fluorescent penetrant indications from the crack in specimen #44. (Part 2 of 2)**

Figure 14. Integrated intensity of fluorescent penetrant indication of crack in specimen #44 normalized to the post-anneal integrated intensity at zero applied stress.

| KSI | Before Annealing | (Mag. 70x) | After Annealing |

Figure 15. Fluorescent penetrant indications from the crack in specimen #53. (Part 1 of 2)

Figure 15. Fluorescent penetrant indications from the crack in specimen #53. (Part 2 of 2)

Figure 16. Integrated intensity of fluorescent penetrant indication of crack in specimen #53 normalized to the post-anneal integrated intensity at zero applied stress.
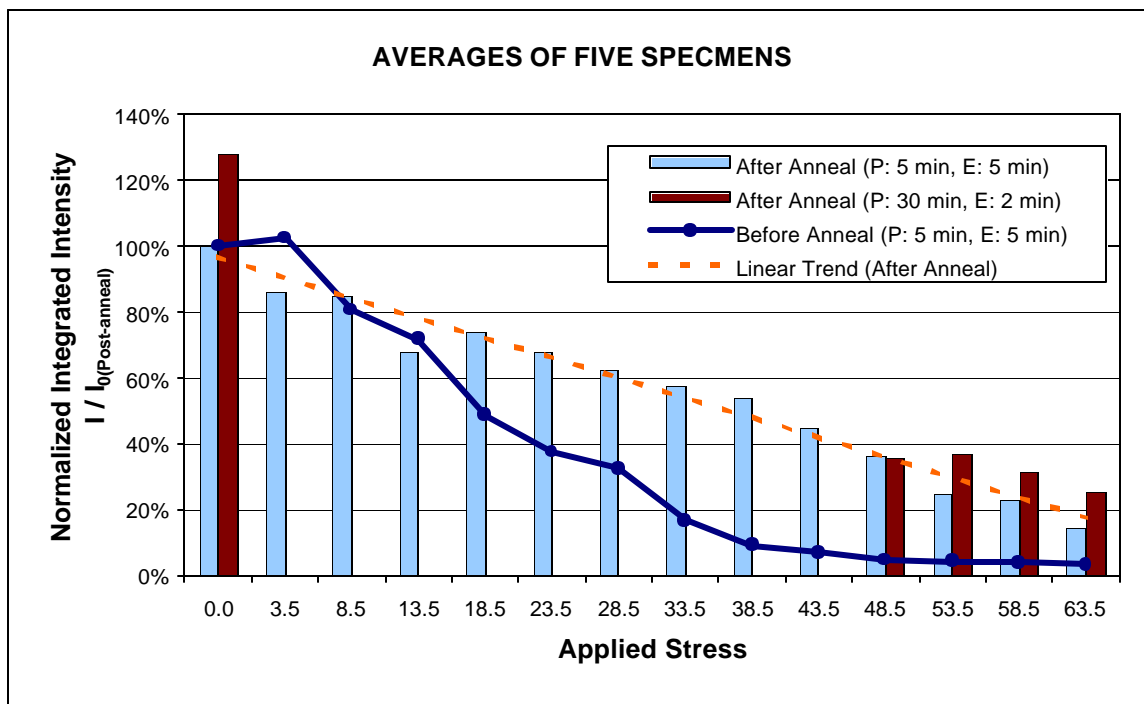
Figure 17. Average integrated intensities of fluorescent penetrant indications versus compressive stress applied to cracked surfaces of the five specimens.
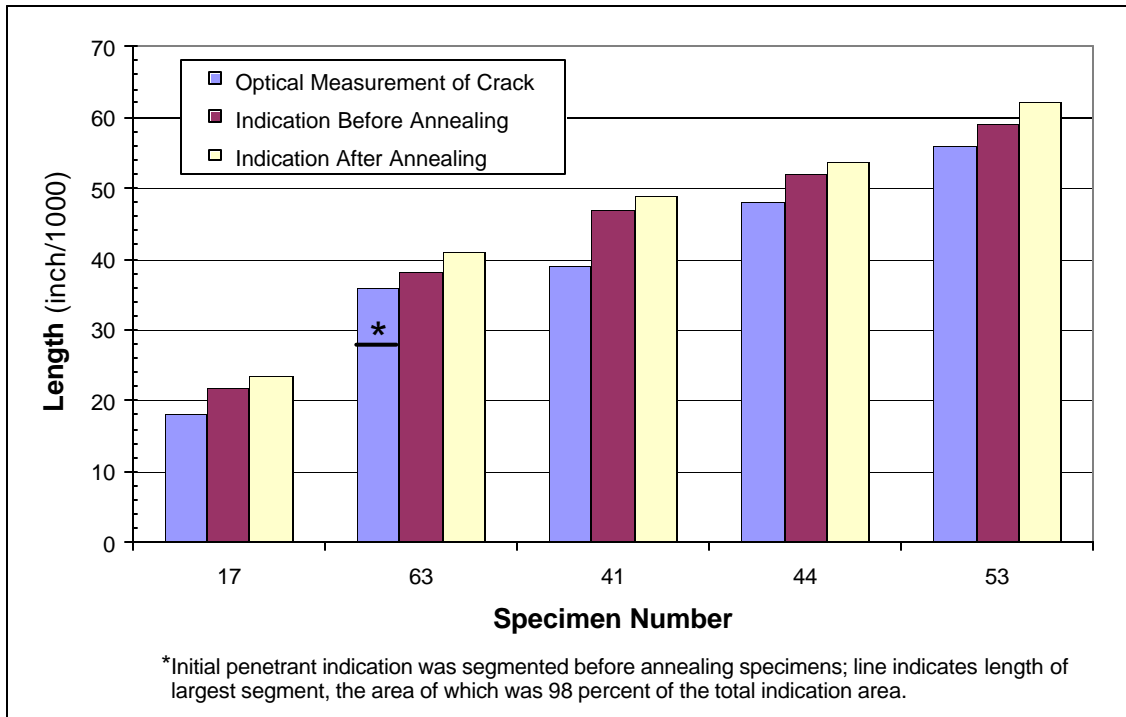
Figure 18. Lengths of fluorescent penetrant indications compared to optically measured crack lengths.
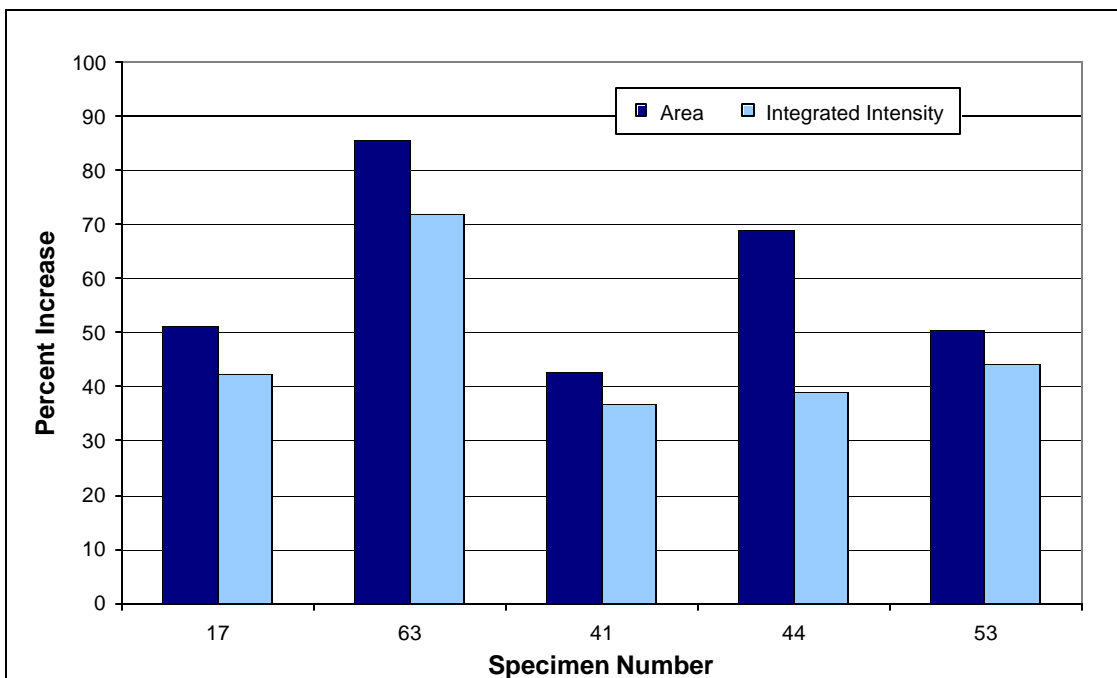

Figure 19. Increases in areas and average intensities at zero applied stress of fluorescent penetrant indications obtained after annealing the cracked specimens compared to indications obtained before annealing.
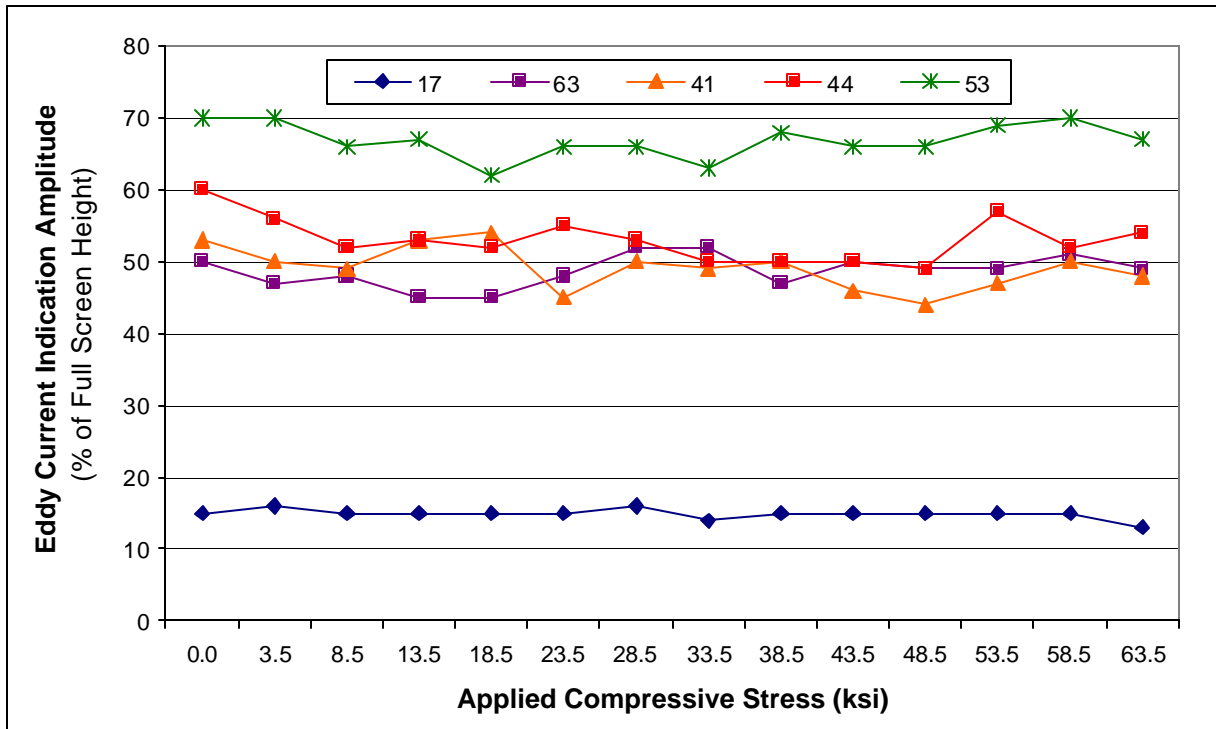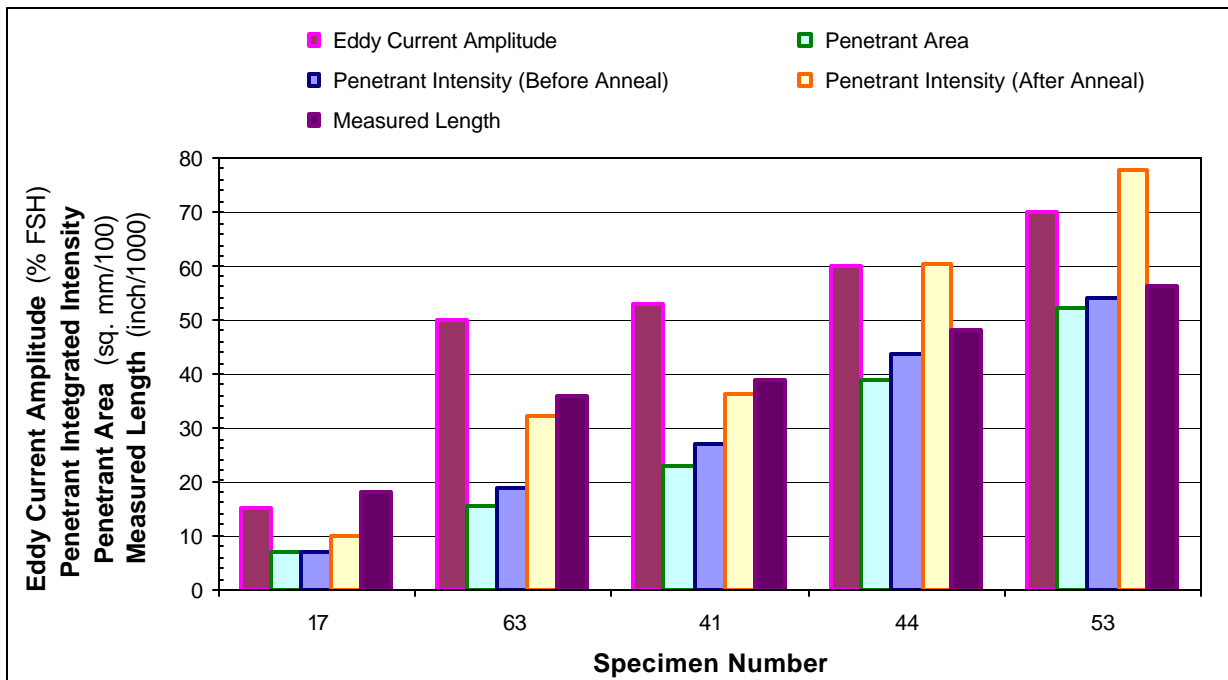
28

Figure 20. Eddy current inspection results.

Figure 21. Comparison of eddy current and penetrant indications with the measured lengths of the fatigue cracks.

---

[1] David G. Moore, Sandia National Laboratories, Airworthiness Assurance NDI Validation Center, Albuquerque, New Mexico.

[2] Aerospace Material Specification, AMS 2644, *Inspection Material, Penetrant*. Warrendale, PA: SAE International (1996).

[3] Ward D. Rummel and George A. Matzkanin, *Nondestructive Evaluation (NDE) Capabilities Data Book*, Third Edition, Nondestructive Testing Information Analysis Center (NTIAC), NTIAC: DB-97-02, (1997)